Microwave circulator based on ferromagnetic nanowires in an alumina template

2010 Nanotechnology 21 145208

(http://iopscience.iop.org/0957-4484/21/14/145208)

Nanotechnology **21** (2010) 145208 (4pp) doi:10.1088/0957-4484/21/14/145208

Microwave circulator based on ferromagnetic nanowires in an alumina template

M Darques[1], J De la Torre Medina[1], L Piraux[1], L Cagnon[2] and I Huynen[3]

[1] Institute of Condensed Matter and Nanosciences, Université Catholique de Louvain, Place Croix du Sud, 1, B-1348 Louvain-la-Neuve, Belgium
[2] Institut Néel, CNRS et Université Joseph Fourier, BP 166, F-38042 Grenoble Cedex 9, France
[3] ICTEAM, Microwave Laboratory, Building Maxwell, 3 place du Levant, B-1348 Louvain-la-Neuve, Belgium

E-mail: michael.darques@uclouvain.be and isabelle.huynen@uclouvain.be

Received 30 October 2009, in final form 9 February 2010
Published 16 March 2010
Online at stacks.iop.org/Nano/21/145208

Abstract
Unbiased planar microwave circulators were fabricated by electrodeposition of NiFe nanowires into porous alumina templates. Microwave properties of the devices are seen to depend drastically on the height of the nanowires and the newly developed devices exhibit improved features, compared to existing nanowire-based designs. Thanks to the high anisotropy of the nanowires, zero-field circulation modes may be observed in a frequency range from 10 to 30 GHz, with isolation as large as 30 dB, as well as low insertion losses −5 dB, making it compatible with industrial needs for device applications.

(Some figures in this article are in colour only in the electronic version)

1. Introduction

On the road towards the size reduction of microwave devices, ferromagnetic nanowires embedded into porous templates have proven to be an interesting alternative route [1] to ferrite-based materials [2]. The main advantages of what we call magnetic nanowired substrates (MNWS) are that they present a zero-field microwave absorption frequency that can be easily tuned over a large range of frequencies [1], as well as being low cost and fast to produce over large areas as compared to standard ferrite devices. Conventional ferrite circulators [3] need to be biased by a magnetic field to operate. This biasing field is generally provided by a permanent magnet and, in view of the volume reduction, much effort was done lately to design unbiased microwave circulators using hexaferrites [4] or ferromagnetic nanowires [5]. Such templates were recently used to design various microwave devices (reviewed in [1]), such as phase shifters [6], isolators [7] or circulators [5]. In this paper, we will discuss a new type of planar integrated microwave circulator of improved design, fabricated on porous alumina templates, as sketched in figure 1(b). In the case of the microwave circulator, although the proof of concept as a first prototype was demonstrated for nanowires embedded into a porous polymer membrane, the fabricated device presented drawbacks [5]. These drawbacks are linked to the nature of the template used. First, polymer membranes are not compatible with cleanroom processes and can therefore not be introduced into the fabrication of a finalized device. More problematic is the fact that such membranes present large dielectric losses [8] leading to huge insertion losses. Finally, due to the large interfacial strain mismatch between polymer and metal it is not possible to deposit metallic layers thicker than a few hundred of nanometers for the ground plane and the microstrip line, leading to important conducting losses. All together, these polymer-based MNWS devices are worthless for industrial applications and research has focused on finding templates suitable for microwave purposes. We present a new type of microstrip microwave circulator based on nanowires embedded into a porous alumina template. Indeed, alumina being known to present low dielectric losses [9], these devices display low insertion losses, close to −5 dB, as well as large isolation, up to 39 dB at 29 GHz. Another advantage compared to polymer

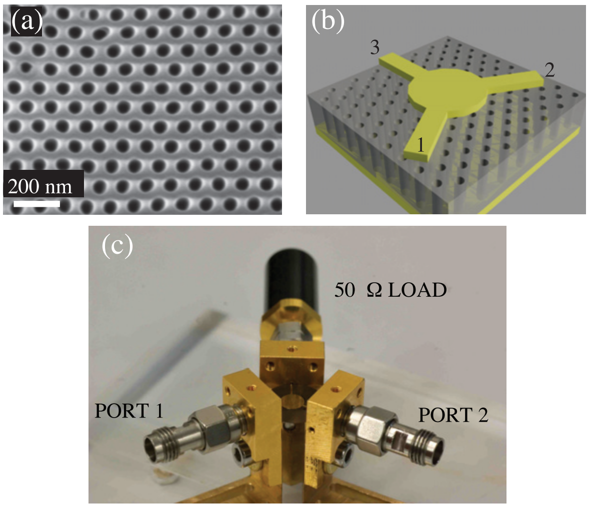

Figure 1. (a) Scanning electron microscope top view of an alumina membrane having pore diameters of 50 nm and porosity 20%; (b) sketch of the microwave circulator, where a metallic disc with three ports is evaporated on one face of the membrane: only the region below the disc is filled beforehand with nanowires; (c) top photograph of an actual device having one port connected to a 50 Ω load.

templates is that alumina may be incorporated into existing cleanroom processes, and microwave circuits have recently been designed on such a substrate by electron beam and optical lithography [10].

2. Experimental details

The template used for fabricating the devices is a porous alumina membrane, done by anodization of a 99.99% pure aluminum foil at a potential of 40 V, using a 0.5 M oxalic acid solution [12]. The pore diameters and interdistance are fixed by the anodization potential, while the membrane thickness depends only on the anodization duration. The resulting templates used in this study are 50 μm and 60 μm thick, with average pore diameter 50 nm and porosity $P = 12\%$ and $P = 20\%$, respectively. P is defined as the product of the pore density times the surface of a single pore, and corresponds to the packing factor of the array. A scanning electron microscope top view of the 60 μm thick, $P = 20\%$ membrane is shown in figure 1(a). NiFe nanowires are grown by electrodeposition into the pores of the alumina membrane using an electrolytic bath of composition $NiSO_4 \cdot 7H_2O$ (1 M), $FeSO_4 \cdot 6H_2O$ (0.05 M) and H_3BO_3 (0.5 M), whose pH is adjusted to 3 by adding concentrated sulfuric acid. Growth of the nanowires, with a ± 1 μm precision in their average length is done in potentiostatic mode by applying a constant potential $E = -1$ V. A circulator is fabricated after the following steps: first the alumina membrane is covered with a 1 μm thick gold layer that will serve as a ground plane as well as a cathode for electrodeposition of the nanowires. Next, NiFe nanowires are deposited in the membrane through a 3 mm mask. Finally, a 3 mm diameter mask (including the three-port accesses) is aligned on top of the region containing the nanowires and a 1 μm thick gold layer is evaporated through this mask to complete the device (see figure 1(b) for a sketch of the device). For microwave characterization of a circulator, two ports are connected to a Vector Network Analyzer (VNA) Model Anritsu 37297C, while the third one is terminated by a 50 Ω load, as shown in figure 1(c).

3. Theoretical modeling

In a recent publication, we have studied the dielectric properties of nanowired substrates by proposing a theoretical permittivity model [11]. Based on a microstrip line approach, it takes into account the filling ratio and the porosity of a porous material. Basically, the air gap between the top of the nanowires and the strip line on top of the membrane is considered to add parallel capacitances to the system. The total effective permittivity is written [11] as

$$\varepsilon_{\text{eff}} = h_{\text{p}} \left(\frac{h_{\text{w}}}{\varepsilon_{\text{w}}} + \frac{h_{\text{a}}}{\varepsilon_{\text{p}}} \right)^{-1}, \tag{1}$$

where h_{p} is the height of the template, h_{w} the length of the nanowires, h_{a} the air gap between the top of the nanowires and the surface of the membrane, and ε_{p} and ε_{w} are the permittivities for the air gap and the nanowire-filled regions, respectively. These are written as

$$\varepsilon_{\text{p}} = P + (1 - P)\varepsilon_b (1 - \text{j} \tan \delta), \tag{2}$$

$$\varepsilon_{\text{w}} = P \left(1 - \text{j} \frac{\sigma_{\text{w}}}{\omega \varepsilon_0} \right) + (1 - P)\varepsilon_b (1 - \text{j} \tan \delta), \tag{3}$$

where j is the imaginary unit, σ_{w} is the conductivity of the wires, $\tan \delta$ the dielectric loss tangent factor of porous alumina and ε_b its dielectric constant.

As presented in figure 2, the permittivity depends linearly on the porosity and increases drastically with the filling of the membrane for filling rates above 50%. Therefore, h_{w} is a parameter that has to be carefully controlled since the resulting variations in permittivity will result in huge variations in effective permittivity and finally in the behavior of the microwave circulator. The modeling of the circulator is done by combining the permeability tensor of the magnetic nanowires embedded in the alumina template, with an analytical formalism [5] derived from that of Bosma [13]. At the remanent state, the permeability tensor $\bar{\bar{\mu}}$ of the composite substrate under the metallic disc (see figures 1(b) and (c)) is [5, 13]

$$\bar{\bar{\mu}} = \begin{bmatrix} \mu & -\text{j}\kappa & 0 \\ \text{j}\kappa & \mu & 0 \\ 0 & 0 & 1 \end{bmatrix}, \tag{4}$$

with

$$\mu_{\text{wire}} = 1 + \frac{h_{\text{w}}}{h_{\text{p}}} P \frac{\omega_m(\omega_m/2 + \text{j}\omega\alpha)}{(\omega_m/2 + \text{j}\omega\alpha)^2 - \omega^2} \tag{5}$$

$$\kappa_{\text{wire}} = \frac{h_{\text{w}}}{h_{\text{p}}} P \frac{\omega_m \omega}{(\omega_m/2 + \text{j}\omega\alpha)^2 - \omega^2}, \tag{6}$$

where $\omega_m = \tilde{\gamma} 4\pi M_S$ with M_S the saturation magnetization, $\tilde{\gamma}$ the gyromagnetic factor, ω the angular pulsation and α the damping factor [5]. It explains why FMR can occur in the

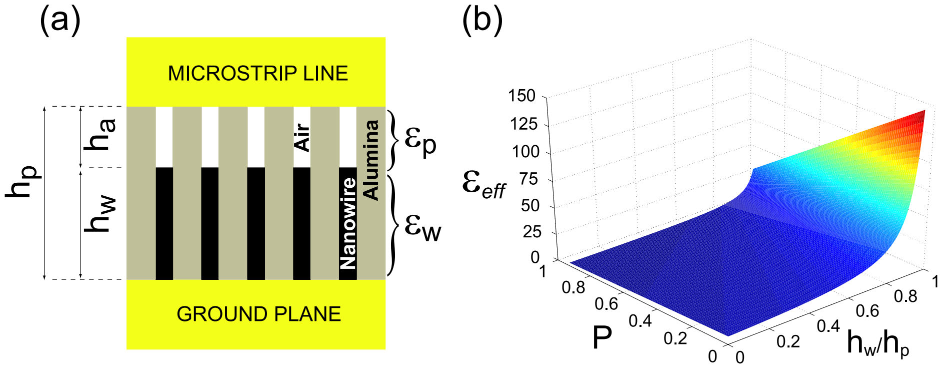

Figure 2. (a) Sketch of the system considered for the analytical permittivity model, showing nanowires embedded into a porous alumina template with gold microstrip line and ground plane and (b) permittivity estimated from the model, depending on the membrane porosity and height of the nanowires.

absence of a DC biasing field, which is mandatory for the operation of circulators without an external field.

The general solution for the component of the electric field E_z normal to the alumina substrate is [13]

$$E_z(r,\phi) = \sum_{n=-\infty}^{+\infty} a_n J_n(k\,r)\mathrm{e}^{\mathrm{j}n\phi}, \tag{7}$$

where J_n is the nth-order Bessel function, r the radial position and ϕ the azimuthal angle, while $k = \omega\sqrt{\varepsilon_0\mu_0\varepsilon_{\mathrm{eff}}(\mu^2-\kappa^2)/\mu}$ is the effective propagation constant inside the disc. The corresponding azimuthal component of the magnetic field intensity $H_\phi(r,\phi)$ is

$$H_\phi(r,\phi) = \sum_{n=-\infty}^{+\infty} \mathrm{j}\frac{a_n}{\zeta_{\mathrm{eff}}}\left[J_n'(kr) - \frac{\kappa}{\mu}\frac{J_n(k\,r)}{k\,r}\right]\mathrm{e}^{\mathrm{j}n\phi}, \tag{8}$$

where $\zeta_{\mathrm{eff}} = \left(\frac{\mu_0(\mu^2-\kappa^2)}{\varepsilon_0\varepsilon_{\mathrm{eff}}\mu}\right)^{1/2}$ is the effective intrinsic wave impedance of the magnetic nanowired substrate. In this latter parameter, $\varepsilon_{\mathrm{eff}}$ is extracted from (1) and we may therefore expect a strong dependence of the circulator behavior on the wires' height. From boundary conditions, it is known that the tangential component of the magnetic field at each connection ($r = \rho = R$) must be equal to the magnetic field in the corresponding microstrip lines forming the accesses to the disc. Combining these boundary conditions with (7) and (8), the impedance matrix of the three-port circulator is derived and then converted into its corresponding scattering matrix. Figure 3 shows the simulated transmission S parameters in a 3 mm diameter circulator on an alumina substrate containing NiFe nanowires. Parameters for the calculation are: M_S = 650 emu cm^{-3}, R = 3 mm and P = 12%. The height of the nanowires compared to the thickness of the membrane is (a) 20%, (b) 50%, (c) 75% and (d) 90% and the respective values of $\varepsilon_{\mathrm{eff}}$, μ and κ are estimated from the model given by (1), (5) and (6). These simulations show that the behavior of the device depends drastically on the filling of the membrane. First, the device must operate with low insertion losses, that is below or above the minimum observed at the same frequency in both S_{21} and S_{12}. It occurs at 28, 22, 16, and 12 GHz for 20, 50, 75 and 90% of the filling height, respectively. Its position indeed depends on the value of k_{eff} in (8), which depends on $\varepsilon_{\mathrm{eff}}$, and hence on filling, as stressed above. Next, the volume of magnetic material must be sufficient to induce isolation; this is at least 20% filling. Indeed a microwave circulator [3] can be basically seen as a 'microwave roundabout', as represented in the sketch in figure 1(b): a microwave signal entering into the device through port 1 may only travel towards port 2, in port 2 towards port 3 and so on. The path 2 → 1 (S_{12}) is thus forbidden, resulting in strong isolation with respect to the path 1 → 2 (S_{21}). More interestingly, the circulation frequency decreases linearly with increasing nanowire height, but in the meantime the isolation of the first circulation reaches a peak at about 75% filling. Therefore, the optimum performance for this device is obtained for wire heights ranging from 50% to 75%.

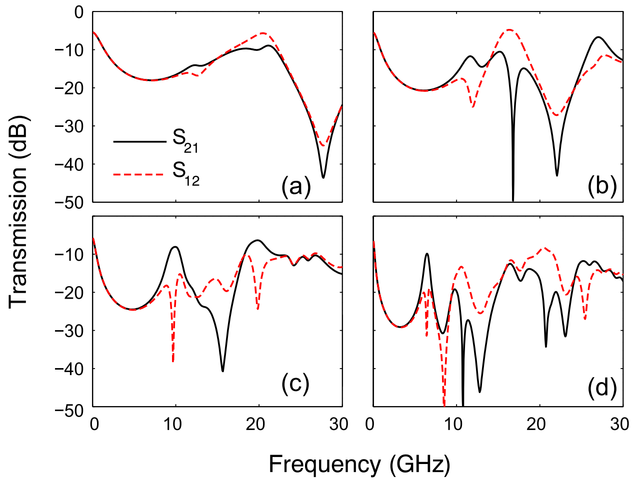

Figure 3. Simulated forward S_{12} and reverse S_{21} transmission for a 3 mm circulator based on NiFe nanowires embedded into a porous alumina template for various heights of the nanowires: (a) 20%, (b) 50%, (c) 75% and (d) 90%. Zero-field resonance frequency of the nanowires is fixed at 12.6 GHz for a membrane porosity, P = 12%.

4. Experimental validation

Prior to the realization of a device, we have characterized the microwave properties of these NiFe nanowires using ferromagnetic resonance [14]. We find that the zero-field

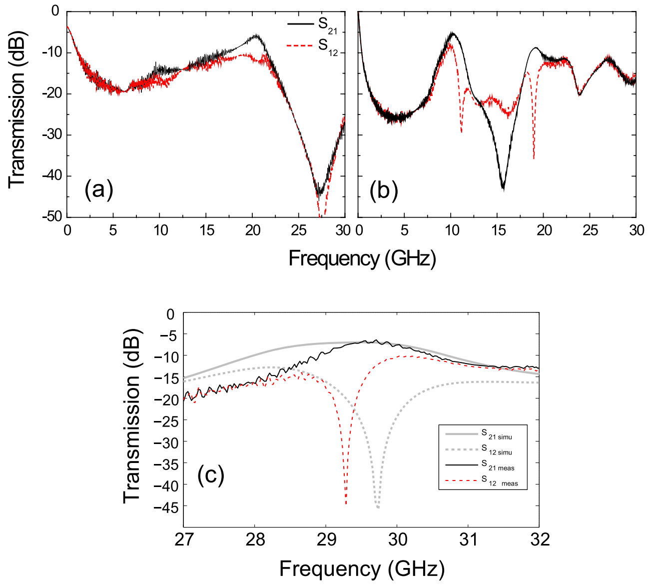

Figure 4. Measured forward S_{12} and reverse S_{21} transmission for a 3 mm circulator based on NiFe nanowires embedded into a porous alumina template for (a) $P = 12\%$, 20% high nanowires and (b) $P = 12\%$, 75% high nanowires. (c) Similar device realized on a $P = 20\%$ template filled with NiFe nanowires over 50% of substrate height.

resonance frequency of an array of NiFe nanowires in the membranes with $P = 12\%$ and $P = 20\%$ is 12.6 GHz and 10 GHz, respectively. This corresponds to $M_S = 650$ emu cm^{-3} and the frequency shift is only due to the difference in dipolar interactions, which are stronger in the $P = 20\%$ template [1]. The analytical model was used to design actual devices. Forward (S_{12}) and reverse (S_{21}) transmission measurements performed on 3 mm devices are shown in figure 4. The first sample (figure 4(a)) is filled with NiFe nanowires up to 20% of the membrane's thickness, and only a very slight circulation effect can be noticed around 20 GHz. The height of the NiFe nanowires for the second sample (figure 4(b)) is 75% of the membrane's thickness. Both measurements are in very good agreement with the simulations presented in figure 3(c). It can be seen that the device presents a large difference in transmission level between (S_{12}) and (S_{21}) at 11 and 19 GHz, which are two distinct circulation modes. Performances show good insertion loss levels of −5 dB and −7 dB at 11 GHz and 19 GHz, respectively, while they both exhibit an excellent isolation of about 25–30 dB.

Performance at a higher frequency may be obtained, using the $P = 20\%$ membrane, yielding a zero-field frequency of 10 GHz as mentioned above. A 3 mm device was fabricated with the wire's height 50% in an alumina template with $P = 20\%$; as seen in figure 4(c), it exhibits a circulation at 29.2 GHz with insertion losses as low as −6 dB and isolation of 35 dB.

5. Conclusions

In conclusion, we have successfully fabricated microwave circulators based on NiFe nanowires embedded into an alumina porous matrix. The circulation performances can be tailored/optimized by an adequate combination of filling height of nanowires and FMR zero-field frequency. Future developments will include the optimization of the metallic pattern shape in order to improve the matching and further reduce insertion losses. As presented, these devices already show excellent performance compared to previous designs, and are a great step towards the transfer of such technology to existing ones. High frequency (>20 GHz) operating circulators may be used in satellite communications and automotive applications (collision avoidance radars).

Acknowledgments

MD and IH are Associate Member and Research Director of FRS/FNRS, respectively. This work was partly supported by the Interuniversity Attraction Poles Program (P6/42)-Belgian State-Belgian Science Policy. Pascal Simon is acknowledged for his help and support in the microwave measurements.

References

[1] Darques M, Spiegel J, De la Torre Medina J, Huynen I and Piraux L 2009 *J. Magn. Magn. Mater.* **321** 2055–65
[2] Harris V G *et al* 2009 *J. Magn. Magn. Mater.* **321** 2035–47
[3] Helszajn J 1969 *Principles of Microwave Ferrite Engineering* (London: Wiley–Interscience)
[4] Queck C and Davis L 2003 *Electron. Lett.* **39** 1595–7
[5] Saib A, Darques M, Piraux L, Vanhoenacker-Janvier D and Huynen I 2005 *IEEE Trans. Microw. Theory Tech.* **53** 2043–9
[6] De la Torre Medina J, Spiegel J, Darques M, Piraux L and Huynen I 2010 *Appl. Phys. Lett.* **96** 072508
[7] Kuanr B K, Veerakumar V, Marson R, Mishra S R, Camley R E and Celinski Z J 2009 *Appl. Phys. Lett.* **94** 202505
[8] Allaeys J-F, Marcilhac B and Mage J-C 2007 *J. Phys. D: Appl. Phys.* **40** 3714–7
[9] Molla J, Gonzalez M, Vila R and Ibarra A 1999 *J. Appl. Phys.* **85** 1727
[10] Spiegel J, Renaux C, Darques M, De la Torre Medina J, Piraux L, Simon P, Raskin J-P and Huynen I 2009 *Proc. 39th European Microwave Conf.* p 582
[11] Spiegel J, De la Torre Medina J, Darques M, Piraux L and Huynen I 2007 *IEEE Microw. Wirel. Compon. Lett.* **17** 492–4
[12] Dahmane Y, Cagnon L, Voiron J, Pairis S, Bacia M, Ortega L, Benbrahim N and Kadri A 2006 *J. Phys. D: Appl. Phys.* **39** 4523–8
[13] Bosma H 1964 *IEEE Trans. Microw. Theory Tech.* **12** 61–72
[14] Darques M, Piraux L, Encinas A, Bayle-Guillemaud P, Popa A and Ebels U 2005 *Appl. Phys. Lett.* **86** 072508